J. Membrane Biol. 5, 51–77 (1971)

Junctional Membrane Permeability

Effects of Divalent Cations

GILBERTO M. OLIVEIRA-CASTRO* and WERNER R. LOEWENSTEIN

Cell Physics Laboratory, Department of Physiology,
Columbia University College of Physicians and Surgeons,
New York, New York 10032

Received 13 January 1971

Summary. Junctional membranes of *Chironomus* salivary gland cells were exposed to test media of varying divalent cation concentration through a hole (estimated diameter $\sim 10\ \mu$) in a cell's nonjunctional surface membrane. Junctional conductance is markedly depressed by Ca^{++}, Mg^{++}, Sr^{++}, Ba^{++} and Mn^{++}. The order of potency is $Ca^{++} > Mg^{++} > Sr^{++} > Ba^{++}$; the minimal effective concentration for Ca is 4 to 8×10^{-5} M. Tests with Ca^{++} show that, at least, this ion also depresses junctional permeability to fluorescein (mol. wt. 330). The permeability depression is confined to the junctional membranes to which (exogenous) Ca^{++} has direct access via the hole. The permeability change produced by Ca^{++} is apparently fast enough to limit transjunctional flux of this ion. The depression is reversed by repolarization of the nonjunctional membrane with inward current when the junctional membrane is exposed to divalent cation-free medium, but not when it is exposed to medium containing 10^{-3} M Ca.

Perforation of the nonjunctional membrane in divalent cation-free medium leads to transient depression of junctional permeability when the membrane hole is large enough to cause nearly complete cell depolarization. This depression can be prevented by clamping the membrane potential with inward current. Smaller holes (estimated diameter $\sim 2\ \mu$) seal in the presence of divalent cations; the ion diffusion barrier is restored within 14 to 30 min of divalent cation application.

Earlier results from this laboratory have shown that the permeability of junctional membrane depends on Ca^{++} (Loewenstein, 1967*a*; Loewenstein, Nakas & Socolar, 1967). In the present work, we study the effects of other divalent cations – Mg^{++}, Sr^{++}, Ba^{++}, and Mn^{++} – and examine the action of Ca^{++} more closely.

Access to the junctional membrane for test substances may be gained by intracellular injection, by breaking the cell-cell seal that shields the

* Ford Foundation and U.S. National Institutes of Health International Fellow. Present address: Institute of Biophysics, Federal University of Rio de Janeiro, Brazil.

external aspect of the junctional membrane from the extracellular environment, or by breaking the nonjunctional surface membrane (Loewenstein, 1966; Loewenstein *et al.*, 1967; Loewenstein, 1967*b*). For the present experiments, we use the last approach; we make a hole in the nonjunctional membrane of one cell of a *Chironomus* salivary gland. This allows exposure of the junctional membrane to media of known ion concentration, as well as interchange of media. Moreover, by restricting nonjunctional membrane alteration to one cell, the method makes it possible to see effects on the junctional membrane alone.

Materials and Methods

Salivary gland cells of 10 to 12-day-old *Chironomus thummi* larvae were used. The procedure for gland isolation and the setup for exchange of media and electrical measurement (and the accuracy of the measurements) were as in the preceding paper of this series (Rose & Loewenstein, 1971). In the four-electrode arrangement (e.g., Fig. 2, inset), one of the current-delivery electrodes (i_R) served to monitor the input resistance of the perforated cell, that is, the resistance between cell interior and exterior determined with both current-passing and voltage-recording electrodes in this cell. In the three-electrode arrangement (e.g., Fig. 6, inset), the current-passing electrode (i_t) used to test coupling was moved to the perforated cell for checking of input resistance during perforation. The resistance of the current-passing electrodes was 8 to 12 MΩ (generally 10 MΩ), and that of the voltage-recording electrodes, 15 to 30 MΩ. The i_t and i_R were inward current pulses of 200 to 350 msec duration (generally 200 msec). Unless stated otherwise, all experiments were performed on giant border cells (G-cells) of the gland (*see* Rose, 1971, for gland morphology, Fig. 2).

The compositions of the control and test media are given in Table 1. The pH of the media was adjusted to 7.40 with NaOH (about 5 mM). In the trials with test media of

Table 1. *Composition of media* (mM)

Medium	KCl	NaCl	Na_2 Fumarate	$CaCl_2$	Mg-Succinate	Glutamine	TES[a]	Na_2 Succinate	Ca Succinate	$MgCl_2$	$SrCl_2$	$BaCl_2$	$MnCl_2$
Control	2	28	28	5	7	80	5						
Ca, Mg-free	2	38	28			68	5	7					
Ca	2	28	28	5		80	5		7				
Mg	2	28	28		7	80	5			5			
Sr	2	28	28			80	5	7			12		
Ba	2	28	28			80	5	7				12	
Mn	2	28	28			80	5	7					12

[a] N-tris-(hydroxymethyl) methyl-2-amino-ethano sulfonic acid.

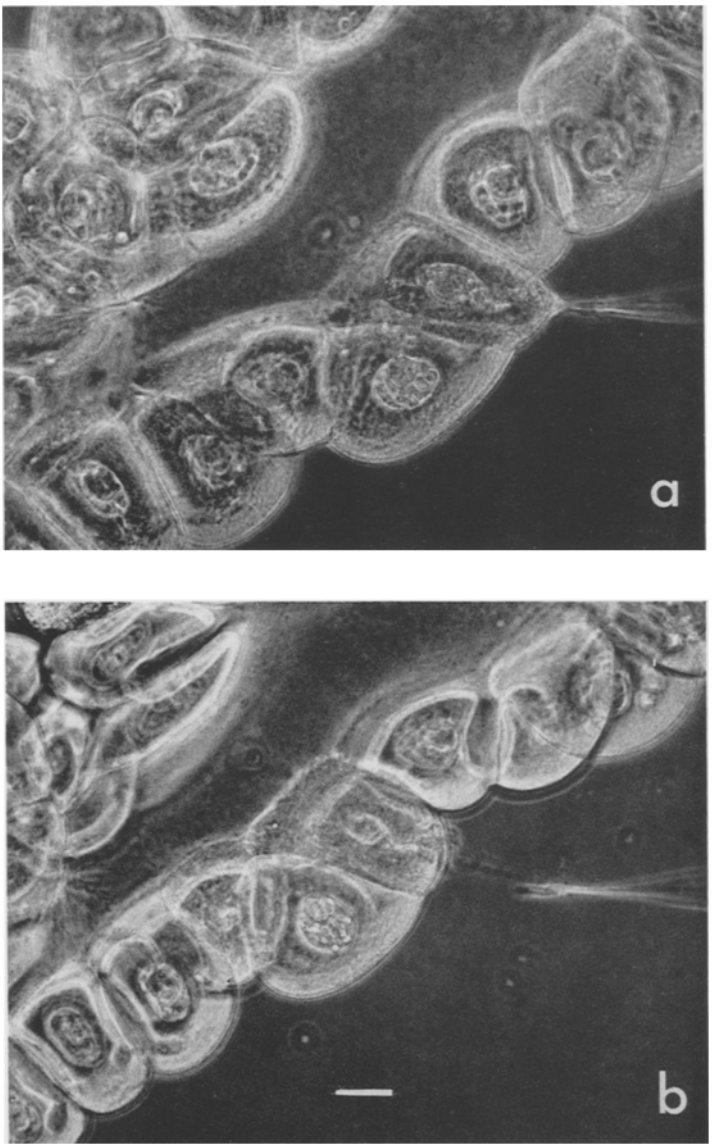

Fig. 1. Cell perforation. Photomicrograph of a living unstained salivary gland, showing the final stages of the drilling of a class A hole in a G-cell. Calibration, 50 μ

varying divalent cation concentration, no compensations for osmolarity or ionic strength were made. All glassware was acid-washed to avoid divalent cation contamination.

In the experiments with phospholipase A (Calbiochem) and trypsin (Mann Research Lab.), the enzymes were dissolved in control medium.

All experiments were done at room temperature ranging from 20 to 25 °C.

Surface Membrane Perforation

The holes in the cell surface membrane were made by moving a micropipette in and out of the membrane until the input resistance of the perforated cell had been reduced to the desired value (Fig. 1). Input resistance was monitored during perforation. The hole was close to cell center, on the average ca. 60 μ away from the G-cell junctions. Inward movement of the pipette was kept to less than 10 μ to minimize damage to intracellular structures. Holes made for the present experiments were in two size ranges, *Class A* holes, made with pipettes of 4 μ tip diameter, gave cell input resistance of <95 KΩ; *Class B* holes, made with 0.5 μ pipettes, gave input resistance of 210 to 400 KΩ. The cell input resistance in the intact cell system was 850 ± 40 (SE) KΩ (50 cases).

Fluorescein Injection

Micropipettes, of about 0.5 μ tip diameter, were first filled with distilled water which was then replaced by a solution, 80 mM in Na_2-fluorescein and 50 mM in KCl, shortly before use. (The pipettes were then kept with tips immersed in a 1:10 or 1:20 dilution of this solution to avoid crystal formation in the tips.) The fluorescein anion was driven out of the pipettes with current pulses (5×10^{-8} amp, 500 msec duration, 1/sec. 2-min, train duration). The procedures for excitation and viewing of fluorescence were as in the experiments of the preceding paper.

Results

Our approach for studying the action of divalent cations on the junctional membrane was to equilibrate the cytoplasm with media of known ion concentration through a hole in a cell's (nonjunctional) surface membrane. This required (*a*) that the perforation by itself produce no major and long-lasting alteration in junctional permeability and (*b*) that the diffusion of divalent cations through the hole be fast relative to their outward membrane transport. Holes of class A (*see* Methods) satisfied these conditions. Holes of class B did not meet condition *b*; they were therefore not useful in testing the effects of divalent cations on junctional membrane. However, the experiments with these holes brought out a phenomenon of interest in itself, that of reconstitution of the cell surface diffusion barrier. We deal first with this phenomenon before describing the effects of divalent cations on junctional permeability.

Nonjunctional Membrane

Sealing Promoted by Ca^{++} and Mg^{++}

Fig. 2A illustrates the results of a typical experiment with a class B hole. The hole was made in one of the cells of a normally coupled gland in Ca, Mg-free medium, reducing the input resistance (R_{II}) to about one third of

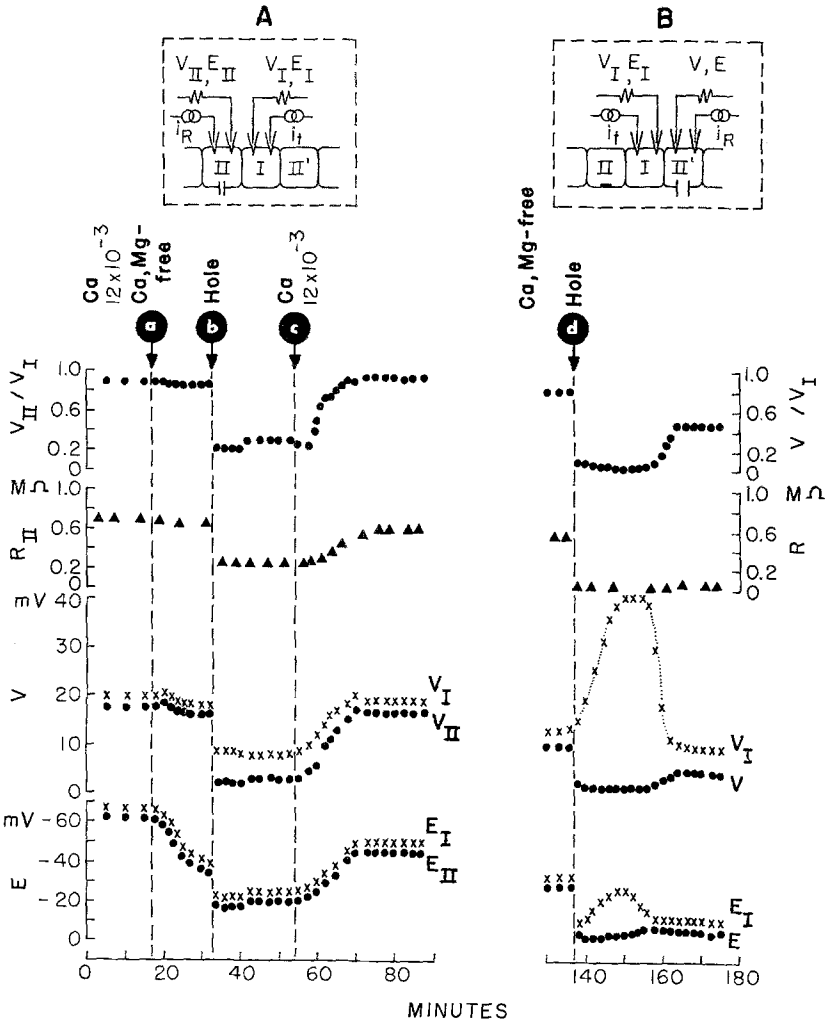

Fig. 2. *A*. Sealing of nonjunctional membrane promoted by Ca^{++}. Test current ($i_t = 2.2 \times 10^{-8}$ amp; 1 pulse/min) is pulsed into cell I, and the resulting potential changes (V) and the potentials at zero current (E resting potential) are recorded in this cell and a contiguous one (II). Independently, current (i_R 0.5 pulses/min) is pulsed into cell II for measurement of input resistance R_{II}. The four electrodes are continuously inside the cells as shown in inset, except during hole drilling. The curves give the time courses of E_I and E_{II}, V_I and V_{II}, the coupling coefficient V_{II}/V_I, and the input resistance R of cell II. Arrow *a* marks exchange of Ca medium ($Ca = 12 \times 10^{-3}$ M) for Ca, Mg-free medium; *b* drilling of a class B hole in cell II; *c* Ca medium, 12×10^{-3} M. *B*. Transient uncoupling following a class A perforation. Same cell system as in *A* after sealing of class B hole in cell II; the second potential recording electrode (and the i_R electrode) is now in cell II′ for measurement of coupling between cells I and II′ and R and E in cell II′. Time base is continuous with that of *A*. *d*, a class A hole is made in Ca, Mg-free medium. $i_t = 2.2 \times 10^{-8}$ amp

the original value. As a result, the resting potential (E) of the perforated cell (II) and of its neighbor (I) fell abruptly to about 20 mV. The cells remained coupled, although the V_{II}/V_I ratio was less than in the intact cell system because of the shunt. The hole stayed open as long as the cells were in Ca, Mg-free medium; R_{II} remained essentially unchanged. When the Ca, Mg-free medium was exchanged for a medium containing 3×10^{-3} M Ca, R_{II} rose progressively almost to its control value in the intact cell system, and the V_{II}/V_I ratio regained its original value. Evidently a diffusion barrier had formed at the membrane hole sealing it off to the ions carrying our current.

Sealing of this kind ensued in all cases tested (10) in which Ca^{++} was present in the medium (Ca concentrations ranged from 1×10^{-3} to

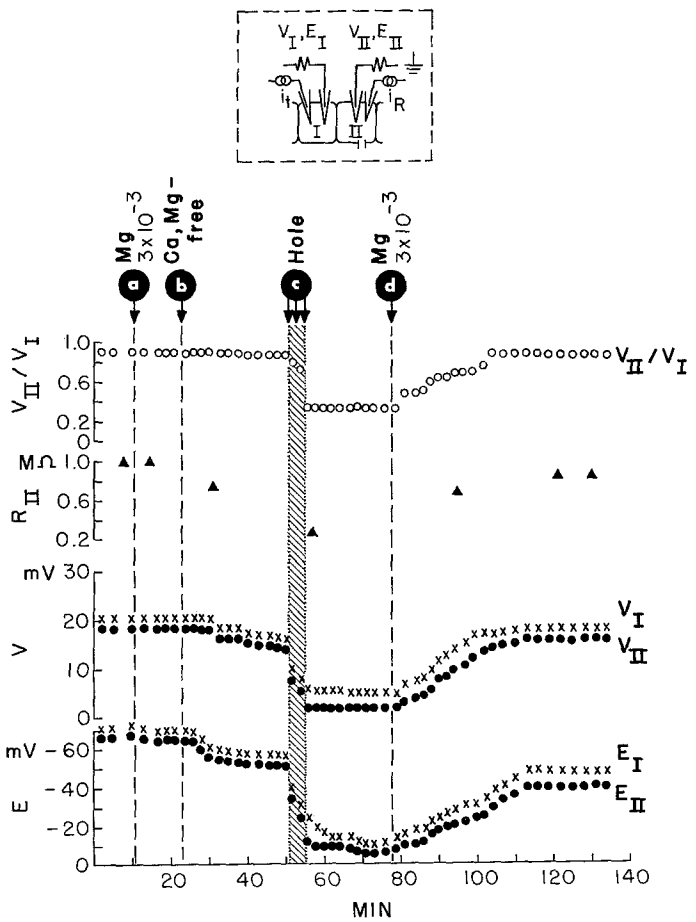

Fig. 3. Sealing of nonjunctional membrane promoted by Mg^{++}. $i_t = 2 \times 10^{-8}$ amp. At *a*, control medium is exchanged for Mg medium (3×10^{-3} M); *b*, Ca, Mg-free medium; *c*, class B hole; the three arrows mark three drilling periods; *d*, Mg medium (3×10^{-3} M)

12×10^{-3} M). The cell input resistance began to rise within 1 to 2 min of Ca^{++} application, reaching within 14 to 30 min a stable maximum value which was 70 to 100% of the original resistance in the intact cell system. The recovery of input resistance was paralleled by a recovery of resting potential to 60 to 90% of the original level (Figs. 2A & 3).

Similar results of sealing were obtained with Mg (1×10^{-3} M) (eight cases) (Fig. 3); Sr (five cases) and Ba (four cases) were not effective (concentration range 1 to 4×10^{-3} M).

Junctional Membrane

Transient Uncoupling

Holes of class A do not seal. These larger holes, which produce at least a one order-of-magnitude drop in cell input resistance, retain their shunt efficacy in Ca or Mg medium. For instance, in the case illustrated in Fig. 11, upon perforation the input resistance of the perforated cell fell from 1,330 to below 15KΩ (the limit of resolution of the method) and stayed below this level in 12×10^{-3} M Ca medium, or, as shown in Fig. 15, with a somewhat smaller perforation lowering input resistance from 840 to 80 KΩ, the input resistance stayed within 15% of the latter value in 12×10^{-3} M Mg medium.

Class A perforation leads to a fall of junctional conductance (*uncoupling*) in Ca, Mg-free medium: V_I rises, while V_{II} falls below detectable level (Figs. 2B & 6). The uncoupling is transient. It starts within 2 min of perforation (often within 1 min) and reaches a peak within 4 to 12 min; stable coupling is restored within 20 to 35 min.

The transient character of this uncoupling was shown most clearly with class A holes which did not excessively shunt the cell interior (e.g., Fig. 2B). A rise in V in cell II′ was then measurable as V_I fell from its peak value; the V/V_I coefficient reached a relatively high value; i.e., junctional conductance once again becomes high.

The transient uncoupling is also reflected in the resting potentials. E_I, which upon perforation had initially fallen together with and to as low a level as E_{II} in the coupled state, rose again as the cells uncoupled. E_I and E_{II} equalized once again as the cells recoupled (Figs. 2B & 6).

The uncoupling following class A perforation and the transient character of this uncoupling are further evident from experiments in which junctional permeability is probed with fluorescein molecules (*see* p. 71).

Uncoupling and Membrane Potential. The transient uncoupling is related to cell depolarization. With class A holes, the perforated cell and its imme-

Table 2. *Cell surface membrane perforation, depolarization and transient uncoupling*

Exp. no.	Hole class	Input resistance (R_{II} [a], KΩ)		Membrane potential (E_{II} [a], mV)		Transient uncoupling
		Intact	Perforated	Intact	Perforated	
0317	A	700	<15	30	0	+
0703	A	700	<15	20	0	+
0704	A	680	45	28	2	+
0714	A	1,040	<15	30	0	+
0715b	A	580	45	20	0	+
0717	A	850	30	40	0	+
0719	A	720	45	26	4	−
0730	A	880	<15	38	0	+
0803b	A	360	15	20	0	+
0806b	A	320	<15	16	0	+
0810	A	1,100	70	32	2	+
0824	A	800	45	40	4	+
0828b	A	400	<15	18	0	+
1015	A	1,000	90	30	2	+
1016	A	900	60	30	4	−
1026	A	820	<15	20	0	+
1028	A	1,130	70	32	2	+
1118	A	700	45	38	4	+
1124	A	620	80	40	2	+
1218	A	680	70	9	0	+
0324	B	640	250	30	12	−
0715a	B	650	260	36	20	−
0729	B	670	260	32	14	−
0803a	B	720	360	45	18	−
0806a	B	880	320	35	16	−
0812	B	1,500	400	42	14	−
0818	B	760	280	50	12	−
0820	B	840	300	28	10	−
0828a	B	820	400	46	20	−
1027	B	900	300	30	12	−

[a] Input resistance and resting potential of cell II before and after perforation in Ca, Mg-free medium; *see* Methods and insets of Figs. 2 and 6 for electrode arrangement. E_I (steady state) is in most cases equal to E_{II} within the resolution of the method; it is, in all cases, within 10 mV of E_{II}.

diate neighbors depolarize. With class B perforations – which do not lead to transient uncoupling – the cells depolarize, too, but the depolarization with class A holes is faster and more complete (Table 2). Moreover, the uncoupling can be prevented by holding the membrane potential of an immediate cell neighbor (intact) with the aid of inward current; or, once begun, the

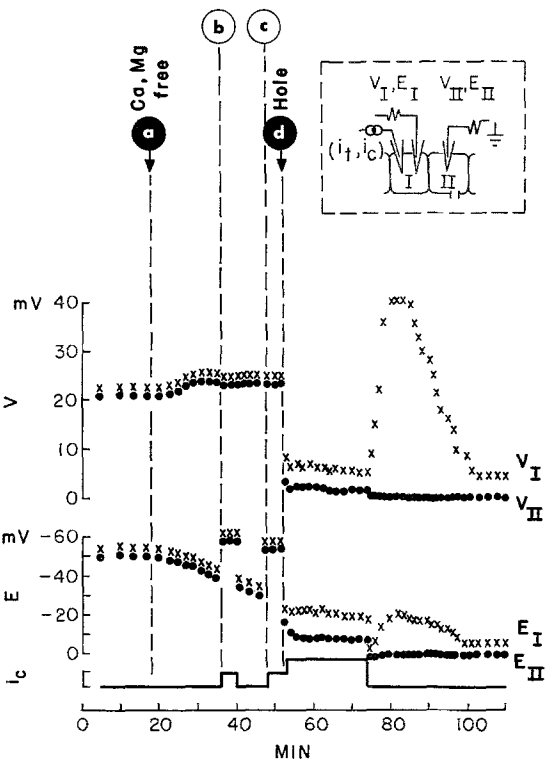

Fig. 4

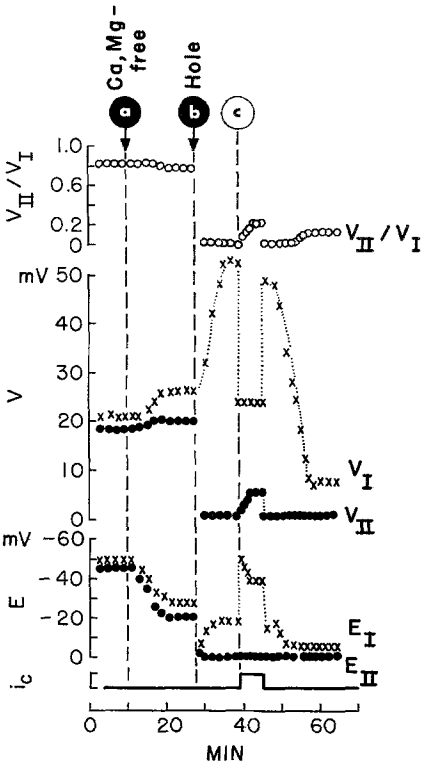

Fig. 5

Fig. 4. Transient uncoupling and membrane potential. *a*, a class A hole is made in cell II (input resistance R_{II} falls from $680 \rightarrow 70$ KΩ) and resting potential of cell I is held around -20 mV after perforation by inward current i_c passed into cell I. The i_c step is started at *c* and adjusted after perforation. *b*, control step of inward current before perforation. i_c calibration, 5×10^{-8} amp. Test current pulses ($i_t = 3.5 \times 10^{-8}$ amp) are superimposed on i_c for measurement of coupling between cells I and II

Fig. 5. Reversal of transient uncoupling during repolarization. Electrode arrangement and general procedure as in Fig. 4. *a*, exchange of control for Ca, Mg-free medium; *b*, class A hole (R_{II}, $820 \rightarrow <15$ KΩ); *c*, application of a step of inward current i_c during the uncoupling phase. $i_t = 2.5 \times 10^{-8}$ amp, i_c calibration, 2×10^{-8} amp

uncoupling can be terminated by raising the membrane potential. In the experiment of Fig. 4, the uncoupling is prevented by holding the membrane potential of cell I at about -20 mV. There is no uncoupling as long as the membrane potential is kept at that level; transient uncoupling develops promptly when the resting potential is allowed to drop to the low level of the potential of the perforated cell. In the example of Fig. 5, uncoupling is abruptly terminated by repolarizing the cell to around -40 mV; the un-

coupling starts again when the resting potential is allowed to drop. By alternating repolarization and depolarization of this sort, one can produce repeated periods of uncoupling.

Effects of Divalent Cations on Junctional Conductance

Persistent Uncoupling

The state of high junctional conductance following the transient uncoupling is maintained for periodsof at least 1 hr in Ca, Mg-free medium. On

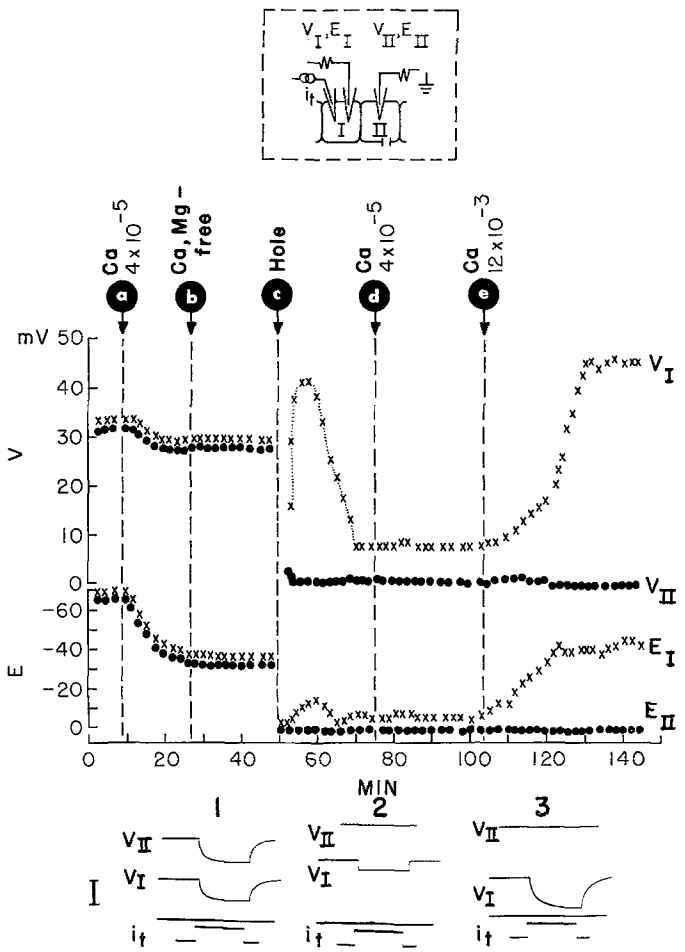

Fig. 6. Effect of Ca^{++} on junctional conductance. *a*, exchange of control for Ca medium (4×10^{-5} M); *b*, for Ca, Mg-free medium; *c*, class A hole (R_{II}. 1,130 → 70 KΩ); *d*, Ca medium (4×10^{-5} M); *e*, Ca medium (12×10^{-3} M). Note the recovery of E_I during transient (*c–d*) and persistent uncoupling (beyond *e*). $i_t = 2.5 \times 10^{-8}$ amp. *Below:* Samples of oscilloscope records of *i* and *V* of a similar experiment (different preparation). *1*, in Ca, Mg-free medium before perforation; *2*, after perforation (after end of phase of transient uncoupling); *3*, 10 min after application of Ca medium. Note the differences in time constants of V_I. $i_t = 2 \times 10^{-8}$ amp, 250 msec. Voltage calibration, 25 mV

this steady state of conductance, we tested the action of divalent cations. The general result was a marked reduction in junctional conductance with ions of the alkaline earth series. Fig. 6 illustrates this for the case of Ca^{++}. One of the cells had been perforated (class A hole) in Ca, Mg-free medium (*c*) and after the transient uncoupling (*c–d*) had taken its course, the cells were exposed first to a medium containing 4×10^{-5} M Ca and then to one containing 12×10^{-3} M Ca. In the presence of the latter, junctional conductance fell as is reflected by the rise of V_I, simultaneous with a fall of V_{II} to below detectable level. (Moreover, the time constant of the V_I pulses, which had fallen markedly during the steady state of high junctional conductance in Ca, Mg-free medium, rose again as cell I uncoupled from the shunted cell neighbor; Fig. 6 *bottom*.)

The result shown in Fig. 6 is quite typical of 18 experiments with Ca^{++}. The uncoupling develops to a maximum within 16 to 35 min of Ca medium application, in most cases within 20 min. As the cells uncouple from their perforated neighbor, their resting potential (E_I, Fig. 6) recovers to a steady

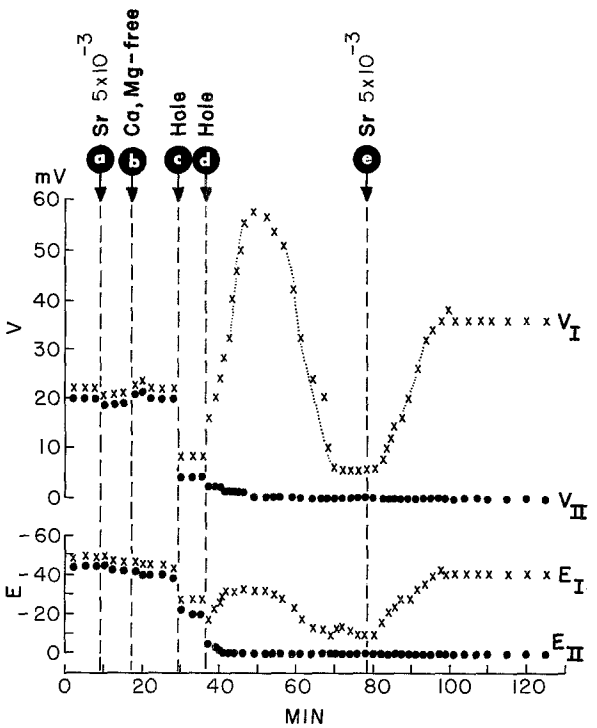

Fig. 7. Effect of Sr^{++} on junctional conductance. Arrangement, procedure and i_t as in Fig. 6. *a*, exchange of control for Sr medium (5×10^{-3} M); *b*, Ca, Mg-free (all-divalent-cation-free) medium; *c*, class B hole (R_{II} 880 → 320 KΩ); *d*, class A hole (R_{II}, 320 → <15 KΩ); *e*, Sr medium (5×10^{-3} M)

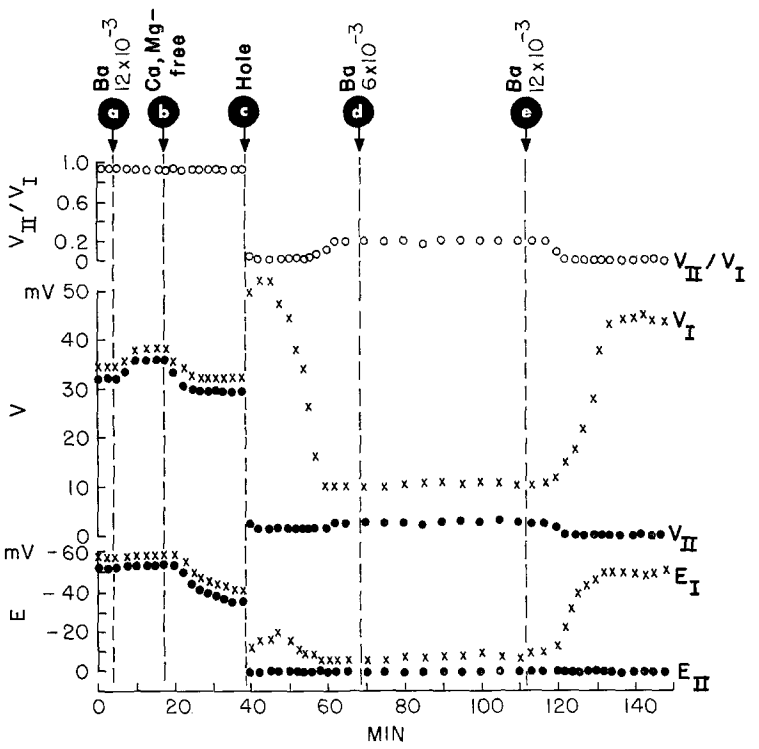

Fig. 8. Effect of Ba^{++} on junctional conductance. Arrangement and procedures as in Fig. 6. $i_t = 3.2 \times 10^{-8}$ amp. *a*, exchange of control for Ba medium (12×10^{-3} M); *b*, Ca, Mg-free medium; *c*, class A hole (R_{II} 1,000 → 95 KΩ); *d*, Ba medium (6×10^{-3} M); *e*, Ba medium (12×10^{-3} M)

and relatively high level, in some instances approaching closely that of the intact cell system (*see* Figs. 7 & 8).

If a class A hole is made directly in Ca medium, uncoupling starts within 2 min and persists (Fig. 12). The transient phase and the persistent uncoupling depending on external Ca^{++} now are presumably superimposed.

The other alkaline earth ions have a similar effect on junctional conductance (Figs. 15A, 7 & 8). However, the potencies of the various ions are quite different. The order of the potencies, as defined by the minimum ion concentration required for uncoupling, is: $Ca^{++} > Mg^{++} > Sr^{++} > Ba^{++}$ (Table 3).

Mn at 1.2×10^{-2} M (the only concentration tested) also produces depression of junctional conductance (Fig. 9).

Uncoupling of G–F and G–G Junction. The giant border cells (G-cells) are connected to each other by direct junction (G–G junction) as well as via the flat cells (F-cells) by junction with these cells (G–F junction; Rose, 1971).

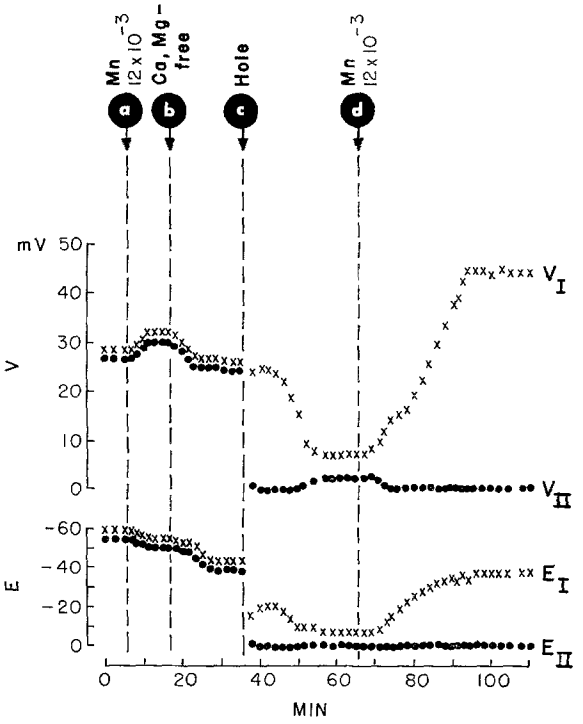

Fig. 9

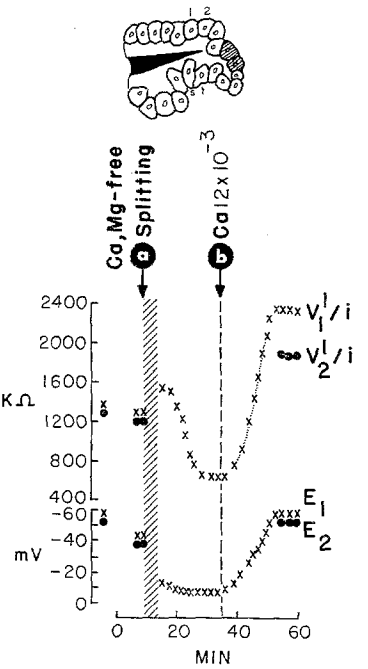

Fig. 10

Fig. 9. Effect of Mn^{++} on junctional conductance. Arrangement and procedures as in Fig. 6. $i_t = 4\times10^{-8}$ amp. *a*, exchange of control for Mn medium (12×10^{-3} M); *b*, Ca, Mg-free medium; *c*, class A hole (R_{II} 620 → 80 KΩ); *d*, Mn medium (12×10^{-3} M)

Fig. 10. Uncoupling of G–F cell junction. Input resistance (V_1^1/i), transfer resistance (V_2^1/i) and membrane potential (E_1, E_2) of two adjacent G-cells. Superscript denotes location of current-passing electrode. At *a*, the gland is partly split by cutting through the F cells in Ca, Mg-free medium. At *b*, Ca medium (12×10^{-3} M) is applied. The points before time zero are the corresponding stable values in Ca medium in the intact gland. Cells on which V/i and E measurements were made are identified with numbers on photomicrograph contour tracing at top. Cut F-cell area in black; damaged G-cells are hatched. Tests for lack of cross coupling were made between lettered and numbered cells

The conductance of both junctions is high relative to that of the nonjunctional surface membrane. The aforedescribed uncouplings, signalled by a substantial rise in V_I, evidently have taken place at both junctions, since otherwise, with either junctional pathway open, much of the current would have been shunted through the hole.

The uncoupling phenomena can, in fact, be demonstrated for each type of junction separately. For the G–F junction, we did this by cutting the F-cells open in Ca, Mg-free medium and measuring subsequently the

input resistance in a G-cell. (It is difficult to make measurements directly in F-cells; these cells are hard to impale with microelectrodes.) In the experiment illustrated in Fig. 10, measurement began 4 min after F-cell injury, in time to record an initial increase in input resistance and then a fall to a stable level much below that in the intact gland (accompanied by a marked fall in the time constant of the pulse of membrane voltage). The phase of increased resistance had a duration of the same order as that of the phase of transient uncoupling caused by G-cell perforation (p. 57). Addition of Ca^{++} during the stable phase of low input resistance raised this resistance above that in the intact gland (Fig. 10) (and the time constant of the pulse of membrane voltage rose again). The current which had been shunted to a large extent through the open F-cell via the G–F junction now flowed through the G-cell surface membrane of high resistance; evidently the G–F junction had sealed itself off.

This uncoupling caused by inflow of Ca^{++} from the F-cell side is restricted to the G–F junction; the G–G junction remains coupled (Figs. 10 & 11). This junction may be uncoupled in a further step, i.e., by perforation (class A) of a G-cell. It is thus easily shown that the G–G junction undergoes a transient fall in conductance when the cells are in Ca, Mg-free media, followed by a persistent fall upon addition of Ca^{++}, or by an immediate persistent fall upon perforation in the presence of Ca^{++}, as in the examples of Figs. 11 & 12. The perforated cell is then uncoupled at all its junctions in Ca medium.

The G–G and the G–F junctions thus show similar reactions to cell perforation and Ca^{++}.

Local Character of Uncoupling. How many in-series junctions are affected by influx of Ca^{++} through a hole in one cell? The gland split along the axis, from the duct up to the G-cell fringe, provided a convenient preparation to examine this question, i.e., a single chain of G-cells. In such a simple array of cells linked by direct junction only, with all cells accessible to electrical measurement, one may get a direct answer by perforating one of the cells in Ca medium and measuring the electrical coupling between the other cells of the chain. Fig. 11 illustrates an example for a chain of six cells with the perforated cell at the center. Typically the uncoupling is confined to the junctions of the perforated cell: intact cells on either side of it remain coupled. Similar results were obtained in two trials with Mg^{++}.

Reversibility of Uncoupling. The fall in junctional conductance produced by Ca^{++}, Mg^{++} or Ba^{++} could not be reversed by exposing the perforated cell system to Ca, Mg-free medium (Fig. 13). Exposures for periods of

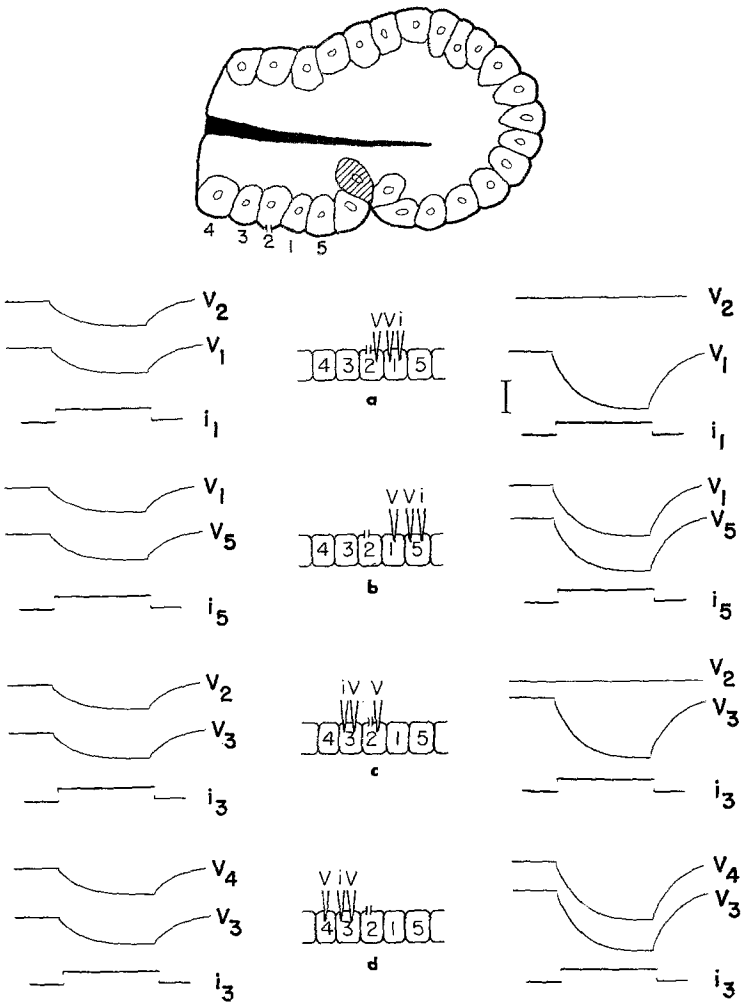

Fig. 11. Local uncoupling. Single chain of six G-cells prepared by splitting of the gland and crushing the seventh cell (chain end). *Top*, contour tracing of the gland; gland split in black, crushed cell hatched. Class A hole was made in cell 2 (R_2, 1,330 → <15 KΩ), and uncoupling was measured serially at cell junctions *a*, 1/2; *b*, 5/1; *c*, 3/2; *d*, 3/4. The corresponding oscilloscope records of *i* (3×10^{-8} amp; 250 msec duration) and of *V* of the measurements before (*left*) and after (*right*) perforation of cell 2 are shown together with a diagram of electrode locations. The *right* records were taken in the order *a–d*; *a* was taken 19 min after perforation (for the complete time course of uncoupling of this junction, *see* Fig. 12). All operations and measurements in Ca medium (12×10^{-3} M). Voltage calibration, 50 mV. The base lines in records *a–d* (*right*) have been shifted to avoid overlap; the *E* values (*left*) are around 50 mV; *E* values (*right*) are

$$E_2 = 0;\ E_1,\ E_5,\ E_3,\ E_4 = 50 \text{ to } 55 \text{ mV}$$

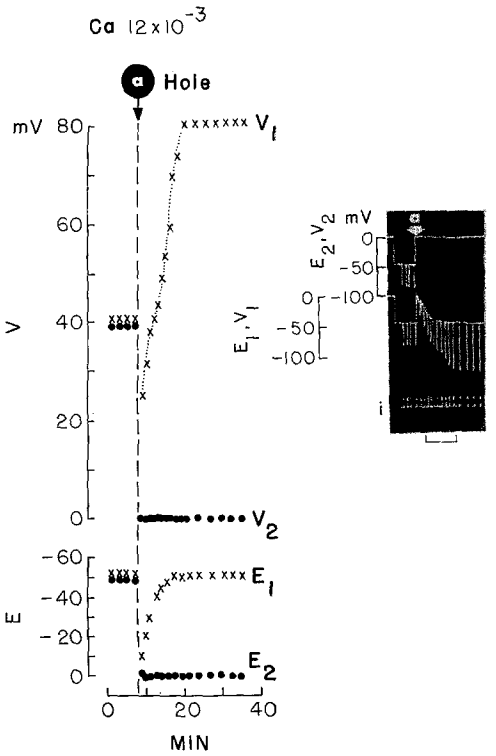

Fig. 12. Uncoupling in Ca medium. Single cell chain. Same cells as in Fig. 11. Time course of uncoupling of G-G junction 1/2 following a class A hole (*a*) in cell 2. (*See* Fig. 11*a*.) *Inset*, storage oscilloscope record on slow time base; the record starts with cell impalement; *V*, downstrokes on the *E* base; *i*, upstrokes. $i_t = 3 \times 10^{-8}$ amp. Time calibration, 7 min

10 to 25 min (to a volume of solution 10^7 times the volume of the cell, frequently renewed) failed to restore coupling of junctions uncoupled by influx of Ca^{++} (nine cases), Mg^{++} (seven cases) and Ba^{++} (four cases). There were signs of reversal in two out of eight trials with Sr^{++}-induced uncoupling.

Restoration of coupling could be produced by cell repolarization in Ca, Mg-free medium. Rose (1970) had found that repolarization by inward current reverses the uncoupling produced in the intact gland by certain metabolic inhibitors or by substitution of Li for extracellular Na. Here repolarization is shown to be equally effective in reversing the uncoupling produced by Ca^{++} influx through a hole. In the examples illustrated in Figs. 13A and B, the membrane potential of one of the cells (I) of an uncoupled cell pair was raised by about 15 mV causing the cells to recouple. The recoupling was particularly clear in the experiment of Fig. 13B where,

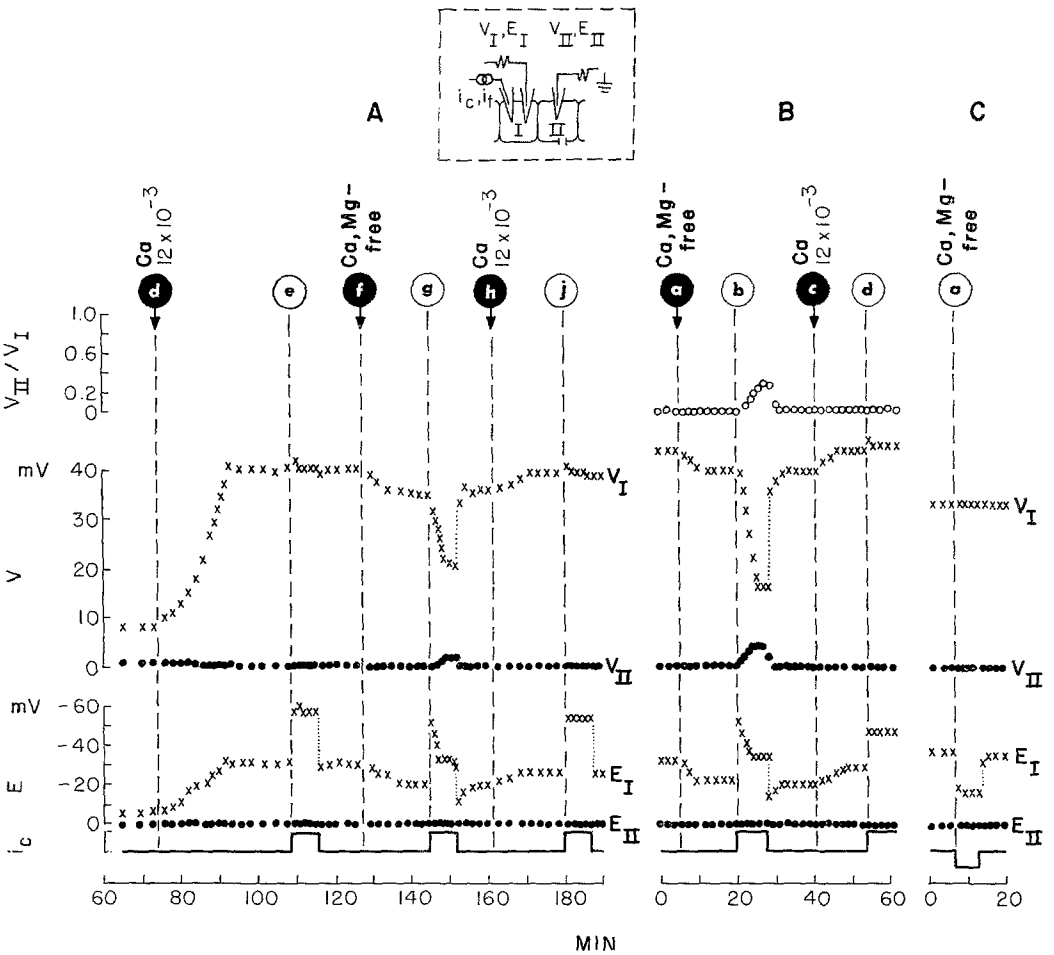

Fig. 13. *A.* Reversal of persistent uncoupling during repolarization in Ca, Mg-free medium. Continuation of experiment of Fig. 5. $i_t = 2.5 \times 10^{-8}$ amp. After completion of the transient phase of uncoupling following the making of a class A hole in Ca, Mg-free medium in cell II (*see* Fig. 5), this medium was exchanged for Ca medium (12×10^{-3} M) (*d*), and during the ensuing steady phase of uncoupling, a step of inward current i_c (i_c calibration, 2.0×10^{-8} amp) is passed in cell I for repolarization (*e*). The Ca medium is then replaced by Ca, Mg-free medium and the same step of current passed again (*g*). *j*, repetition of repolarization in Ca medium. *B.* The cells here (another gland) have undergone the operations *a* and *b* of Fig. 5 and operation *d* of *A*. $i_t = 2 \times 10^{-8}$ amp. The record starts during the steady phase of uncoupling in Ca medium (12×10^{-3} M). At *a*, the Ca medium is replaced by Ca, Mg-free medium, and a step of inward current, as in *A*, is passed to repolarize cell I (*b*). At *d*, the repolarization is repeated in Ca medium (12×10^{-3} M). Note the relatively large increase in V_{II} at *b*; the class A hole here (R_{II} 700 → <15 KΩ) presumably is a smaller shunt than the hole in the case of Fig. 13A. Before perforation, E_I and E_{II} were about −40 mV, V_I was 28 mV, and V_{II} 26 mV. *C.* The cells of this gland underwent the same experimental sequences as the cells in B. R_{II} 680 → 45 KΩ; $i_t = 1.5 \times 10^{-8}$ amp. The cells were then exposed to Ca, Mg-free medium; the record starts in this medium. At *a*, a step of outward current is passed to depolarize cell I

upon repolarization, V_I not only fell to about as low a level as when the cell had been perforated in Ca, Mg-free medium, but V_{II} increased substantially, in spite of the current shunt in cell II. Uncoupling ensued again when the resting potential was allowed to drop.

The reestablishment of a high junctional conductance by repolarization occurred only when the perforated cell system was equilibrated with Ca, Mg-free medium. It did not occur in media containing Ca (3 to 12×10^{-3} M) (Figs. 13A & B) or Mg (6 to 12×10^{-3} M), nor did it occur when the cells were depolarized by outward current (Fig. 13C). (The currents used for repolarization and depolarization ranged from 1.5 to 4.5×10^{-8} amp, 4 to 8 min duration.)

The current-V_I and current-V_{II} relationships are linear over the entire range used in Ca, Mg-free medium (Fig. 14). This is true regardless of whether the relationships are determined at resting potential (Fig. 14A) or on a level of membrane potential raised by inward current maintained for several min (Fig. 14B) as in the case of the above experiments on recoupling by repolarization.

Nonlocal Uncoupling. Exposure of fresh intact glands to Ca, Mg-free medium causes no substantial alteration of coupling for periods of 1 hr and longer (Rose & Loewenstein, 1971). The change from control to Ca, Mg-free medium had two kinds of short-term

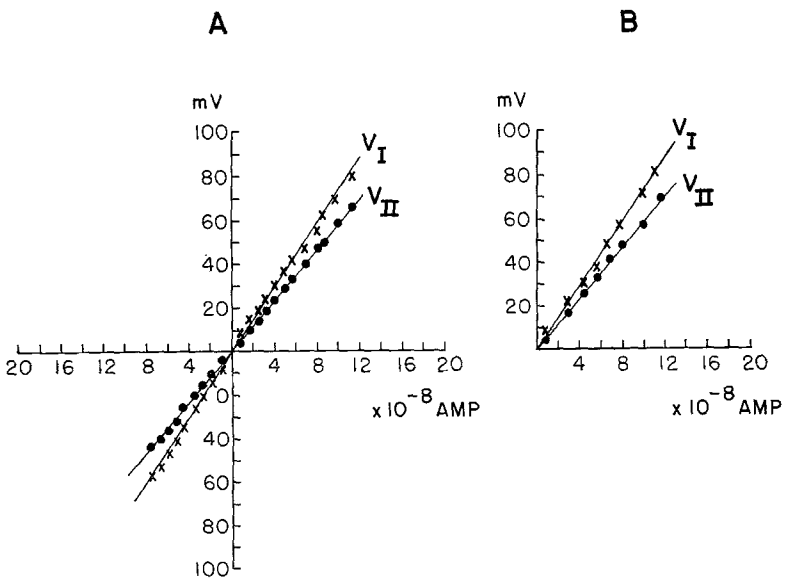

Fig. 14. Current-voltage relation. Intact cells in Ca, Mg-free medium. *A*. Steady-state voltages produced by test pulses of inward (*right*) and outward (*left*) current. Resting potential = −40 mV. *B*. Steady-state voltages produced by test pulses of inward current superimposed, as in the experiments of Fig. 13, on a step of inward current ($i_c = 2.4 \times 10^{-8}$ amp) raising the resting potential from 38 to about 68 mV. Electrode arrangement, test-pulse duration (250 msec), and current-step duration (ca. 8 min) as in Fig. 13. The slopes of the curves in *A* and *B* are identical (V_I slope 7.5×10^5 Ω; V_{II} slope 5.8×10^5 Ω)

effects on cell input resistance: (1) a fall of resistance of the order of 100 KΩ (e.g., Figs. 2, 3 & 6); or (2) a rise of the same order (e.g., Figs. 4 & 5). We believe that in the first case only nonjunctional surface membrane is affected. This behavior falls into line with the well-known one of skeletal muscle, nerve and red blood cells that lack communicative junctions. It was also the response to Ca, Mg-free medium when a given gland cell here had been uncoupled from all its neighbors by their perforation in Ca medium. The second kind of response may possibly be caused by resistance rises in remote junctions. In any event, whatever the differences in this respect, all the aforedescribed results concerning cell performation and the action of divalent cations held for all cases.

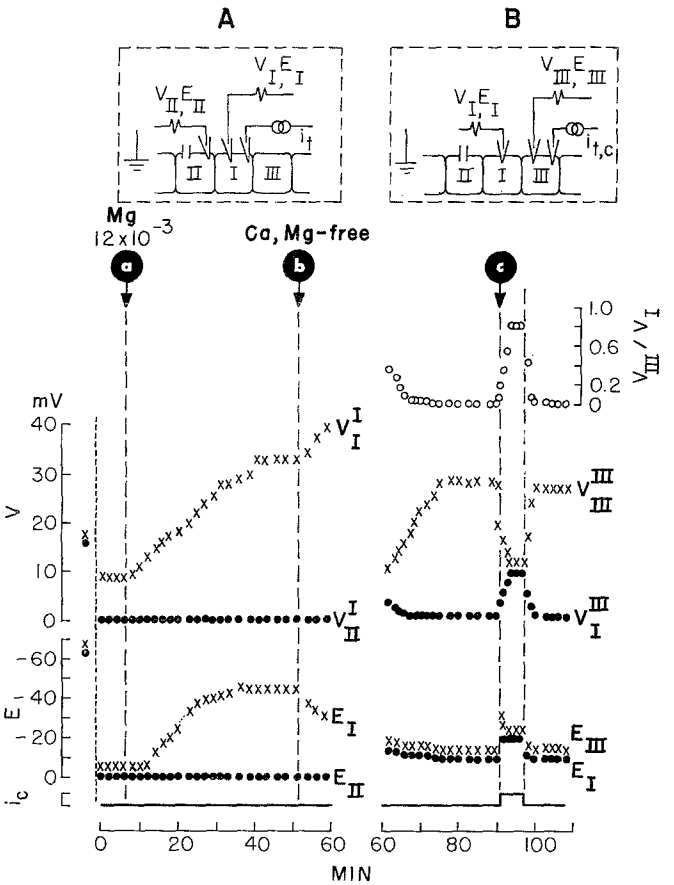

Fig. 15. Nonlocal uncoupling. *A*. A class A hole was made in cell II in Ca, Mg-free medium (R_{II} 840 → 80 KΩ). The curve starts 20 min after the end of the ensuing transient uncoupling of cell I from II. The points before time zero give the V and E values before perforation. (*a*) Ca, Mg-free medium replaced by Mg medium (12×10^{-3} M). During the plateau of the ensuing persistent uncoupling of cell I from II, Ca, Mg-free medium was applied (*b*). Note the new rise in V_I. *B*. The V_{II} and i_t electrodes were then moved to III, in time to follow the uncoupling of cell I from III (time = 60 to 75 min). (*c*) Recoupling of these two cells upon repolarization of cell III with inward current i_c. i_c calibration, 4×10^{-8} amp. $i_t = 2.3 \times 10^{-8}$ amp. Superscripts on the V curves refer to location of the current-passing electrode

When application of Ca, Mg-free medium followed the uncoupling of a junction by influx of divalent cations through a hole, there was, in some cases, uncoupling of additional junctions. With the electrode arrangement of Fig. 15A, this uncoupling manifested itself by a further rise in V_1, beyond the plateau reached after the uncoupling by the influx of divalent cation (b). That this indeed reflects uncoupling of additional junction is shown by the experiment of Fig. 15B in which the electrodes were moved to straddle the next cell junction, in time to follow the fall in its conductance. Further exploration of the cell system showed that many cells, if not all, had then uncoupled.

This general uncoupling occurred in preparations which had been subjected to long periods of experimentation including exposure to Ca, Mg-free medium. It is probably the same kind of general uncoupling caused by prolonged exposure to Ca, Mg-free medium, dealt with in the preceding paper of this series (Rose & Loewenstein, 1971). The experiments on recoupling by repolarization described in the preceding section were all done on preparations which did not show such general uncoupling in Ca, Mg-free medium (*see* Fig. 13).

Permeability to Fluorescein

The preceding experiments were concerned with the permeability of the junctional membrane to the small cellular inorganic ions that carried the electrical current. In the following experiments, we probe the junctional membrane with a larger ion, fluorescein (mol. wt. 330), under the same experimental conditions.

Fig. 16 illustrates an example. Fluorescein was first injected into a cell of the intact gland. The fluorescent tracer spread from one cell interior to another without visible leakage to the exterior (*a*). After 20 min, a class A hole was made in a cell adjacent to the injected one in Ca, Mg-free medium; after the resulting transient "electrical" uncoupling had elapsed, a second injection of fluorescein was made. (By that time – 50 min after the first injection – the fluorescence from this injection was far below the sensitivity of the photographs.) Fluorescein spread again through the cell system, but now it leaked out visibly at the hole (*b*). After the cells had lost their fluorescence[1], the Ca, Mg-free medium was replaced by Ca medium, a hole was made also in the cell on the other side, and fluorescein was injected again. Fluorescein no longer passed beyond the boundaries of the injected cell (*d*).

A variation of this experiment showed the local character of this block for fluorescein (Fig. 17): one cell was perforated and fluorescein was injected in the two immediate neighbors. Here, after application of Ca medium, fluorescein passage is blocked at the junctions with the perforated cell, but

1 Loss of fluorescence in the perforated cell system is rapid; no fluorescence was visible 8 min after injection. With comparable loadings of intact glands, clearly visible levels of fluorescence are present after more than 30 min (the sensitivity of our photographs is very much lower than the visual sensitivity).

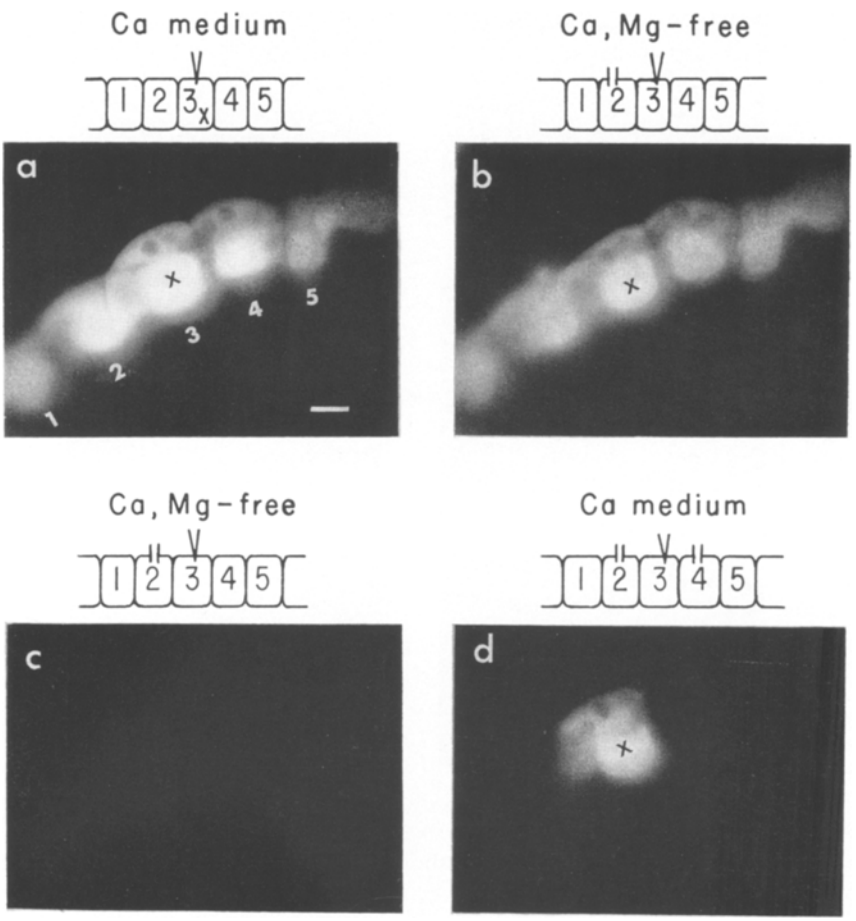

Fig. 16. Effect of Ca^{++} on junctional permeability to fluorescein. (*a*) Intercellular flow in the intact cell system. Cell *3* (cross) was injected with a single 2-min train of fluorescein pulses, and the fluorescence was photographed 6 min thereafter. Cells in Ca medium (12×10^{-3} M). (*b*) 20 min later, the cells' fluorescence having diminished below photographic sensitivity, a class A hole was made in cell *2* and the injection in *3* repeated after the transient phase of uncoupling. The photograph is taken 2 min after the injection. Note the fluorescein leakage through the hole in cell 2. (*c*) Photographed 8 min after the second (*b*) injection; cells are in Ca, Mg-free medium in (*b*) and (*c*). (*d*) The Ca, Mg-free medium was exchanged for Ca medium (12×10^{-3} M), a hole was now made also in cell 4, and after 10 min cell *3* was injected with fluorescein as in (*a*) and (*b*). Dark field photomicrographs; photographic exposure 2.5 min. Calibration, 50 μ

not at the junctions with the intact cells (the intact cells retain fluorescence under these conditions as well as in the fully intact gland; *see* footnote [1]).

In another set of experiments, fluorescein was injected within 3 to 8 min of the perforation, during the transient phase of uncoupling, as determined

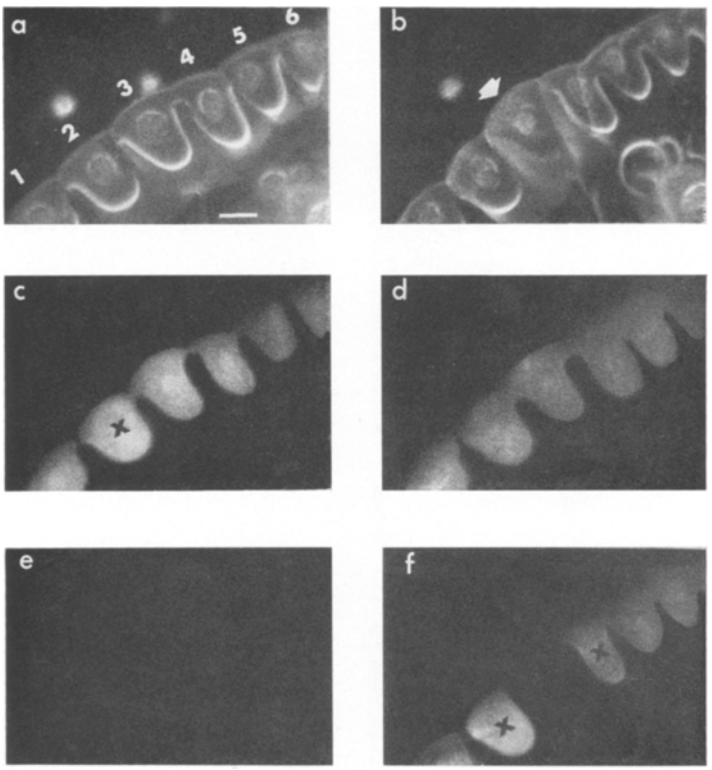

Fig. 17. Ca^{++} effect on fluorescein permeability. Local uncoupling. (*a*) and (*b*) Photomicrograph of cell system in oblique illumination (no blue filter) showing the outlines of the cells. (*a*) intact cells; (*b*) after perforation (arrow) of cell 3 in Ca, Mg-free medium. Hole is not visible in photograph, but note blurring of contours of perforated cell. (*c*)–(*f*) Photomicrographs in dark field with filters for viewing of fluorescence only. A 2-min train of fluorescein pulses is injected in cell *2*, 35 min after perforation, well after transient uncoupling; the fluorescence is photographed 3 min (*c*), 5 min (*d*) and 7 min (*e*) after injection. Cells are in Ca, Mg-free medium from (*a*)–(*e*). The medium is then exchanged for Ca medium (12×10^{-3} M), and 10 min and 13 min thereafter, cells *2* and *4*, respectively, are injected with fluorescein. Fluorescence is photographed 3 min after injection of cell *4*; exposure times (*c*), (*d*), (*e*), 2 min; (*f*), 3 min. Calibration, 50 μ

electrically. Fluorescein then did not pass from the injected cell to the perforated one; it passed when the transient electrical uncoupling had elapsed.

In summary, fluorescein passes from the interior of one cell to another in the intact cell system. If one of the cells is perforated (class A hole) in Ca, Mg-free medium, the passage between the intact and perforated cell is blocked for 4 to 30 min after perforation. Thereafter, the passage is resumed and continues for long periods if the interior of the perforated cell is equili-

brated with Ca, Mg-free medium. The passage is blocked persistently if the interior of the perforated cell is exposed to Ca medium. This block is typically confined to the junctions with the perforated cell; passage between intact cells is generally unimpaired.

The effects of cell perforation and Ca^{++} on intercellular transfer of fluorescein thus closely parallel the effects on transfer of small inorganic ions.

Discussion

Sealing of the Surface Membrane

Impalement of a cell membrane on a 0.5 μ thick micropipette, followed by withdrawal – a common event in electrobiological measurement – usually produces no persistent leak in the membrane. Evidently the membrane hole closes rapidly. The rapid closure is probably caused mainly by elastic membrane forces like those that keep the membrane-pipette junction tight during pipette insertion. This closure is independent of Ca^{++} or Mg^{++} in the medium.

The holes of classes A and B, made by repeated pipette insertion, exceeded the size limits for this kind of closure. We have no histological picture of these holes, but one may get an idea of their size from the value of their conductance. The resistance through a shunting hole is, to a first approximation, the convergence resistance of a circular disk electrode joining two semi-infinite media. The diameter of the hole is then ρ/R, where ρ is the specific resistance of the medium (ca. 100 Ωcm) and R is the convergence resistance of the hole (*cf.* Mason & Weaver, 1929). In cell systems with class A holes, the input conductance is at least one order of magnitude higher than in the intact cell system; hence the final input conductance is attributable entirely to the hole. Thus for a class A hole of 80 KΩ, as in the experiment of Fig. 9, the diameter is on the order of 10 μ. The size of a class B hole may be similarly estimated on the assumption that the final input conductance is the sum of the input conductance of the intact cell system and the conductance of the shunting hole. For a class B hole, as in Fig. 2A, where the hole resistance, 300 KΩ, is half the final input resistance, the diameter is on the order of 2 μ.

Our results show that the class B holes seal in the presence of Ca^{++} and Mg^{++}. The restoration of the diffusion barrier to small ions is complete or nearly complete. The sealing here is different from the hole closure following a single retraction of a fine micropipette; it depends on Ca^{++} or Mg^{++} in the medium. The sealing is probably akin to Heilbrunn's (1927) "surface

precipitation reaction" that prevents escape of cytoplasm from punctured sea urchin eggs in the presence of Ca^{++} or Mg^{++}. There are no data in Heilbrunn's experiments to show if the reacting egg cell surface is also a barrier to small ions, but this seems to be so because the punctured cells survive. In addition, there are several reported instances of membrane sealing in protozoans (*see* Heilbrunn, 1956) and glia cells (Kuffler & Potter, 1964).

We have no positive clues as yet on how Ca^{++} and Mg^{++} promote membrane sealing. One possibility is that the sealing is mediated by membrane lipids. Phospholipid films are known to coalesce, and the coalescence is promoted by Ca^{++} and Mg^{++} (Blioch, Glagoleva, Liberman & Nenashev, 1968). Our work in this direction so far shows only that treatment of the perforated cell system with phospholipase A (0.05 mg/ml) or with trypsin (up to 0.2 mg/ml) does not prevent the sealing induced by Ca^{++}.

Junctional Membrane

The present results reveal that all divalent cations of the alkaline earth series cause marked depression of junctional membrane permeability. In line with an earlier hypothesis concerning the action of Ca^{++} (Loewenstein 1966, 1967*a*), we interpret the permeability depression as caused by binding of the ions to the junctional membrane.

The order of potency for depression, $Ca^{++} > Mg^{++} > Sr^{++} > Ba^{++}$ (Table 3), corresponds to the order of their apparent affinities with barnacle muscle membrane (Hagiwara & Takahashi, 1967; Ba^{++} not tested), with

Table 3. *Uncoupling efficacy of divalent cations*

Ion	Minimum effective concn.[a] (M)	Relative potencies
Ca	$4-8\times10^{-5}$ (3, 5)	1
Mg	$1.2-6\times10^{-4}$ (3, 3)	0.07 – 0.7
Sr	$3-5\times10^{-3}$ (4, 4)	0.008 – 0.027
Ba[b]	$0.7-1\times10^{-2}$ (3, 3)	0.004 – 0.009

[a] The second figure is the minimum tested concentration which elicited uncoupling; the first, the nearest ineffective concentration tested; in parentheses, the respective number of tests at this concentration. (Not included in this tally are the cases tested at higher concentrations, all of which produced uncoupling: Ca^{++}, 12 cases; Mg^{++}, 11 cases; Sr^{++}, 7 cases; Ba^{++}, 6 cases).

[b] The significance of the Ba^{++} data is clouded by the impurity assay which gives a limit of Ca + Sr (as chlorides) contamination as 0.1% by weight in the $BaCl_2$ used.

G-actin (Kasai & Oosawa, 1968), and with their order of potency for blocking negative charge on amphoteric colloids such as casein, G-actin and lecithin (Bungenberg de Jong, 1949; *see* also Diamond & Wright, 1969; *see* also Abramson, Katzman, Gregor & Lurei, 1966, for binding of Ca^{++} and Mg^{++} to phosphatidic acid). The difficulty in reversing permeability depression due to divalent cations by exposure to divalent cation-free medium suggests strong binding of these ions to the junctional membrane as did the experiments with chelators of the preceding paper.

The depression of junctional membrane permeability is restricted to the cell junctions to which exogenous Ca^{++} has direct access through the hole. When the hole is made in Ca medium (Fig. 12), the transient uncoupling presumably precedes the buildup of exogenous Ca^{++} at the junction. This alone may then suffice to limit junctional passage of this ion and thus to prevent propagation of the permeability change to other junctions. However, the permeability depression was confined even when junctional membrane was exposed to exogenous Ca^{++} only after the transient uncoupling (in Ca, Mg-free medium) had elapsed, as well as in a case of class A perforation in which transient uncoupling was exceptionally absent (Table 2, exp. no. 0719). Thus, the permeability transformation by exogenous Ca^{++} appears to be fast enough to limit transjunctional flux of this ion.

This result is different from one obtained earlier indicating that junctions beyond those of the damaged cell can be uncoupled by exogenous Ca^{++} (Loewenstein *et al.*, 1967, Fig. 14). However, the experimental situations are not readily comparable: the holes represented a large area of surface membrane destruction in the earlier experiments, and a different control medium was used in which cells displayed much lower resting potentials and deteriorated faster than in the present exeriments.

The permeability depression produced by the divalent cations is reversed by repolarization of the nonjunctional membrane, as it is in the case of depression produced by metabolic inhibitors and by substitution of Li for extracellular Na (Rose & Loewenstein, 1971). The present result obtained with an open cell system, in which the Ca^{++} environment could be controlled on one side of the junction, is particularly instructive because it demonstrates a relationship between the recoupling phenomenon and $[Ca^{++}]$ that is not immediately apparent from the earlier results obtained on a closed system: the recoupling by repolarization ensues when the $[Ca^{++}]$ of the junctional environment is low, but not when it is high (Fig. 13). The recoupling may be interpreted, with the same argumentation as in the preceding paper (pp. 41–46), as a consequence of restoration of the Ca^{++}-holding capacity of the nonjunctional membrane during repolarization;

that is, this membrane becomes a sink for Ca^{++} ions during repolarization. The sink's effectiveness for drawing Ca^{++} off the junctional membrane will depend ultimately on the $[Ca^{++}]$ in the perforated cell; there is net Ca^{++} loss from junctional membrane only if the $[Ca^{++}]$ in the cell is sufficiently low. In this light, the situation here of recoupling by repolarization in a cell system open to medium of low $[Ca^{++}]$ is analogous to that of recoupling by repolarization in the intact cell system whose internal $[Ca^{++}]$ has been raised critically to the level for uncoupling by metabolic inhibitors or by substitution of Li^{+} for external Na^{+}. The interpretation presupposes, as already discussed (Rose & Loewenstein, 1971), that Ca is exchangeable between the two intracellular sides of a membrane junction.

The transient uncoupling following class A perforation, which is clearly dependent on nonjunctional membrane potential, may be explained along similar lines. During such perforation, the distribution of membrane Ca shifts as the nonjunctional membrane potential approaches zero. The junctional membrane, which before the perforation was in equilibrium with an intracellular environment of low $[Ca^{++}]$, now takes up Ca^{++} released from the depolarizing nonjunctional membrane (or other intracellular storage sites) and, consequently, undergoes a fall in permeability. If the perforation occurs in medium of low $[Ca^{++}]$, the *status quo ante* is soon restored at the junctional membrane by Ca^{++} sequestering action of mitochondria and other intracellular structures. In medium of high $[Ca^{++}]$, mitochondria are swamped with Ca and irreversibly damaged (Wojtczak & Lehninger, 1961; Vasington & Murphy, 1962; Judah *et al.*, 1965); uncoupling is persistent.

We thank Dr. S. J. Socolar for helpful discussion, and Messrs. R. Hatchett and C. Freites for technical assistance and for constructing some of the electronic and mechanical devices used in the present work.

The work was supported by research grants from the National Institutes of Health and the National Science Foundation.

References

Abramson, M. B., Katzman, R., Gregor, H., Lurei, R. 1966. The reaction of cations with aqueous dispersion of phosphatidic acid. Determination of stability constants. *Biochemistry* **5**:2207.

Blioch, Z. L., Glagoleva, J. M., Liberman, E. A., Nenashev, V. A. 1968. A study of the mechanism of quantal transmitter release at a chemical synapse. *J. Physiol.* **199**:11.

Brink, F. 1954. The role of calcium in neural processes. *Pharmacol. Rev.* **6**:243.

Bungenberg de Jong, H. G. 1949. *In*: Colloid Science, vol. II. H. R. Kruyt, editor. p. 259. Elsevier, New York.

Délèze, J. 1970. The recovery of resting potential and input resistance in sheep heart injured by knife of laser. *J. Physiol.* **208**:547.

Diamond, J. M., Wright, E. M. 1969. Biological membranes: The physical basis of ion nonelectrolyte selectivity. *Annu. Rev. Physiol.* **31**:581.

Hagiwara, S., Takahashi, K. 1967. Surface density of calcium ions and calcium spikes in the barnacle muscle fiber membrane. *J. Gen. Physiol.* **50**:583.

Heilbrunn, L. V. 1927. The colloid chemistry of protoplasm. *V.* A preliminary study of the surface precipitation reaction of living cells. *Arch. Exp. Zellforsch.* **4**:246.

— 1956. The Dynamics of Living Protoplasm. p. 62. Academic Press Inc., New York.

Judah, T. D., Ahmed, K., McLean, A. E. M., Christie, G. S. 1965. Uptake of magnesium and calcium by mitochondria in exchange for hydrogen ions. *Biochim. Biophys. Acta* **94**:452.

Kasai, M., Oosawa, F. 1968. The exchangeability of actin-bound calcium with various divalent cations. *Biochim. Biophys. Acta* **154**:520.

Kuffler, S. W., Potter, D. 1964. Glia in the leech central nervous system: Physiological properties and neuron-glia relationship. *J. Neurophysiol.* **27**:290.

Loewenstein, W. R. 1966. Permeability of membrane junctions. *Conf. on Biol. Membranes: Recent Progress. Ann. N.Y. Acad. Sci.* **137**:441.

— 1967*a*. Cell surface membranes in close contact. Role of calcium and magnesium ions. *J. Colloid Interface Sci.* **25**:34.

— 1967*b*. On the genesis of cellular communication. *Develop. Biol.* **15**:503.

— Nakas, M., Socolar, S. J. 1967. Junctional membrane uncoupling. Permeability transformations at a cell membrane junction. *J. Gen. Physiol.* **50**:1865.

Mason, M., Weaver, W. 1929. The Electromagnetic Field. p. 242. University of Chicago Press, Chicago.

Politoff, A. L., Socolar, S. J., Loewenstein, W. R. 1969. Permeability of a cell membrane junction. Dependence on energy metabolism. *J. Gen. Physiol.* **53**:498.

Rose, B. 1970. Junctional membrane permeability: Restoration by repolarizing current. *Science* **169**:607.

— 1971. Intercellular communication and some structural aspects of membrane junctions in a simple cell system. *J. Membrane Biol.* **5**:1.

— Loewenstein, W. R. 1971. Junctional membrane permeability: Depression by substitution of Li for extracellular Na, and by long-term lack of Ca and Mg; Restoration by cell repolarization. *J. Membrane Biol.* **5**:20.

Vasington, F. D., Murphy, T. V. 1962. Ca^{++} uptake by rat kidney mitochondria and its dependence on respiration and phosphorylation. *J. Biol. Chem.* **237**:2670.

Wojtczak, L., Lehninger, A. L. 1961. Formation and disappearance of an endogenous uncoupling factor during swelling and contraction of mitrochondria. *Biochim. Biophys. Acta* **51**:442.